Hindawi Publishing Corporation
International Journal of Antennas and Propagation
Volume 2015, Article ID 989517, 11 pages
http://dx.doi.org/10.1155/2015/989517

Research Article

Joint Phased-MIMO and Nested-Array Beamforming for Increased Degrees-of-Freedom

Chenglong Zhu, Hui Chen, and Huaizong Shao

School of Communication and Information Engineering, University of Electronic Science and Technology of China, Chengdu 611731, China

Correspondence should be addressed to Chenglong Zhu; zhuchenglong01@126.com

Received 18 June 2014; Revised 7 December 2014; Accepted 18 January 2015

Academic Editor: Hang Hu

Phased-multiple-input multiple-output (phased-MIMO) enjoys the advantages of MIMO virtual array and phased-array directional gain, but it gets the directional gain at a cost of reduced degrees-of-freedom (DOFs). To compensate the DOF loss, this paper proposes a joint phased-array and nested-array beamforming based on the difference coarray processing and spatial smoothing. The essence is to use a nested-array in the receiver and then fully exploit the second order statistic of the received data. In doing so, the array system offers more DOFs which means more sources can be resolved. The direction-of-arrival (DOA) estimation performance of the proposed method is evaluated by examining the root-mean-square error. Simulation results show the proposed method has significant superiorities to the existing phased-MIMO.

1. Introduction

In recent years, multiple-input multiple-output (MIMO) has received much attention [1–4]. Many of MIMO superiorities are fundamentally due to the fact that it can utilize the waveform diversity to yield a virtual aperture that is larger than the physical array of its phased-array counterpart [5–8]. However, MIMO array misses directional gain selectivity. In contrast, phased-array has good direction gain but without spatial diversity gain. To overcome these disadvantages, intermediates between MIMO and phased-array are investigated by jointly exploiting their benefits [9–11]. Particularly, a transmit subaperturing approach was proposed in [11] for MIMO radar. The basic idea is to form multiple transmit beams which are steered toward the same direction [12]. In [9], the authors proposed a phased-MIMO technique, which enjoys the advantages of MIMO array without sacrificing the main advantages of phased-array in coherent processing gain. That is to say, phased-MIMO array offers a tradeoff between conventional phased-array and MIMO array.

However, the number of degrees-of-freedom (DOFs) is important criteria because more DOFs mean more sources can be resolved by the system. To compensate the sacrificed DOFs of phased-MIMO radar, it is necessary to increase the DOFs in the receiver. In earlier works, the problem of increasing the DOFs of linear arrays has been investigated in [13, 14], but the augmented covariance matrix is not positive semidefinite anymore. The authors of [14] increase the DOFs with the minimum redundancy arrays [15] and constructing an augmented covariance matrix. Nonuniform and sparse array arrangements are also widely employed [16–21]. Solutions based on genetic algorithm [22, 23], random spacing [24], linear programming [25], and compressive sensing [26–28] have been proposed for phased-array thinning. But sparse array elements have the drawbacks of generating grating lobes. Moreover, it is not easy to extend them to any arbitrary array size. To mitigate these weaknesses, the authors of [29–31] propose a nested-array based on the concept of difference coarray [32], but there are no studies on the joint transmit and receive array design.

Inspired by the phased-MIMO [9] and nest-array [29], this paper proposes a joint phased-array and nested-array beamforming based on the difference coarray processing and spatial smoothing for increased DOFs and consequently more sources can be resolved. The main contribution of this work can be summarized as follows: (1) a joint phased-array

and nested-array beamforming is proposed. This approach optimally utilizes the advantages of MIMO, phased-array, and nested-array and overcomes their disadvantages. (2) Adaptive beamforming based on the spatial smoothing algorithm is presented to resolve the coherent noise problem caused by the difference coarray processing. (3) The direction-of-arrival (DOA) estimation performance of the proposed joint phased-array and nested-array beamforming is extensively evaluated by examining the root-mean-square error (RMSE).

The rest of this paper is organized as follows. In Section 2, we briefly introduce some background on the basic phased-MIMO and nested-array technique. In Section 3, the formulation and signal model of the joint phased-MIMO and nested-array are proposed. It can significantly increase the system DOFs, which means more interferences/targets can be suppressed/identified. Next, Section 4 develops the adaptive beamforming with a spatial smoothing algorithm. Section 5 performs extensive simulations to evaluate the proposed method in DOA estimation by examining the RMSE performance. Finally, conclusions are drawn in Section 6.

2. Preliminaries and Motivations

In this section, we provides an overview of basic phased-MIMO and nested-array.

2.1. Phased-MIMO. The main idea of the phased-MIMO is to divide the M transmit elements into $1 \le K \le M$ subarrays, which are allowed to overlap. All elements of the k $(1 \le k \le K)$ subarrays are used to coherently emit the signal $\phi_k(t)$ in order to form a beam towards an interesting direction. At the same time, different waveforms are transmitted simultaneously by different subarrays.

The complex envelope of the signals emitted by the kth subarray can be modeled as

$$s_k(t) = \sqrt{\frac{M}{K}}\phi_k(t)\,\widetilde{\mathbf{w}}_k^*, \quad k = 1, \ldots, K, \tag{1}$$

where $\widetilde{\mathbf{w}}_k$ is the $M \times 1$ unit-norm complex vector which is comprised of M_k (number of elements used in the kth subarray) nonzero and $M - M_k$ zeros and $(\cdot)^*$ is the conjugate operator. The $\sqrt{M/K}$ is used to obtain an identical transmit power constraint.

The signal reflected by a target located at angle θ in the far-field can then be modeled as

$$r(t,\theta) = \sqrt{\frac{M}{K}}\alpha(\theta)\sum_{k=1}^{K}\mathbf{w}_k^H\mathbf{a}_k(\theta)\,e^{-j\tau_k(\theta)}\phi_k(t), \tag{2}$$

where $\alpha(\theta)$ is the target coefficient and $\mathbf{w}_k$ and $\mathbf{a}_k(\theta)$ are the $M_k \times 1$ beamforming vector and transmit steering vector, respectively. And $\tau_k(\theta)$ is the required signal propagation for the kth subarray. The reflection coefficient $\alpha(\theta)$ for a target is assumed to be constant during the whole pulse but varies from pulse to pulse; that is, it obeys the Swerling II target model [33].

Denoting

$$\mathbf{c}(\theta) \doteq \left[\mathbf{w}_1^H\mathbf{a}_1(\theta), \mathbf{w}_2^H\mathbf{a}_2(\theta), \ldots, \mathbf{w}_K^H\mathbf{a}_K(\theta)\right]^T, \tag{3a}$$

$$\mathbf{d}(\theta) \doteq \left[e^{-j\tau_1(\theta)}, e^{-j\tau_2(\theta)}, \ldots, e^{-j\tau_K(\theta)}\right]^T, \tag{3b}$$

with $(\cdot)^T$ being the transpose operator. Supposing that a target is located at θ_s and D interferences at θ_i, $1 \le i \le D$, for an N-element receive array we can get $KN \times 1$ data vector:

$$\begin{aligned}\mathbf{y} = {} & \sqrt{\frac{M}{K}}\alpha_s(\theta_s)\,\mathbf{u}_{\text{pa-mimo}}(\theta_s) \\ & + \sum_{i=1}^{D}\sqrt{\frac{M}{K}}\alpha_i(\theta_i)\,\mathbf{u}_{\text{pa-mimo}}(\theta_i) + \mathbf{n},\end{aligned} \tag{4}$$

where $\widetilde{\mathbf{n}}$ is the $KN \times 1$ noise term. The $KN \times 1$ virtual steering vector is

$$\mathbf{u}_{\text{pa-mimo}} = [\mathbf{c}(\theta) \odot \mathbf{d}(\theta)] \otimes \mathbf{b}(\theta), \tag{5}$$

where $\odot$ and $\otimes$ denote the Hadamard product and Kronker product, respectively. And $\mathbf{b}(\theta)$ is the $N \times 1$ actual receive steering vectors associated with the direction θ.

It can be noticed from (5) that phased-MIMO radar is a compromise between MIMO and phased-array radar and thus enjoys the advantages of MIMO radar extending the array aperture by virtual array and phased-array radar allowing for maximization of the coherent processing gain through transmit beamforming [34]. From (4), we can conclude that the complexity of the traditional processing algorithm is $O(K^4N^2L)$.

It would be specially mentioned that if $K = 1$ is chosen, then the signal model (4) simplifies to the signal model for the conventional phased-array radar. On the other hand if $K = M$ is chosen, the signal model (4) simplifies to the signal model for the MIMO radar. Thus we can conclude that the degrees of freedom can be got from aforementioned radar system as

$$\text{DOF}_{\text{pa-array}} = N + 1, \tag{6a}$$

$$\text{DOF}_{\text{pa-mimo}} = N + K, \tag{6b}$$

$$\text{DOF}_{\text{mimo}} = N + M. \tag{6c}$$

2.2. Nested-Array. The number of sources that can be resolved by an N-element ULA phased-array using conventional subspace-based methods is $N - 1$. However, according to the difference coarray scheme [32], the maximum attainable number of DOFs, denoted by DOF_{max}, is

$$\text{DOF}_{\text{max}} = N(N-1) + 1. \tag{7}$$

Certainly, if a difference occurs more than once, it implies a decrease in the available DOFs. Consider a linear array with d being the minimum spacing of the underlying grid and define the function $c[m]$ which takes a value 1 if there is an element

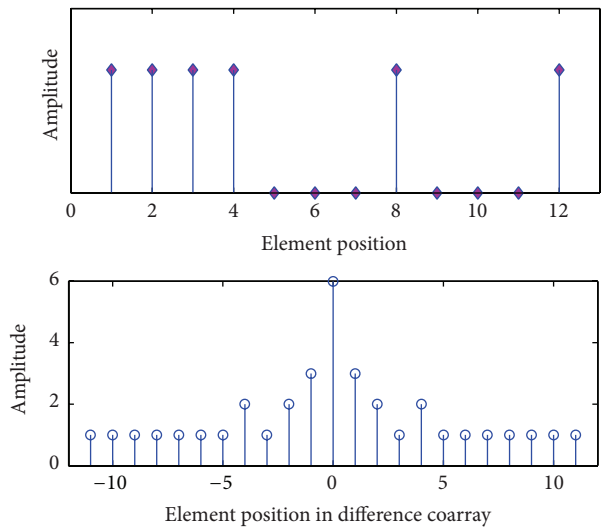

Figure 1: Illustration of a two-level nested-array with $N_1 = 3$ and $N_2 = 3$.

located at md and 0 otherwise. The number of same occurrences in each position, denoted by γ, can be expressed as

$$\gamma = c[m] \circledast c[-m], \tag{8}$$

where $\circledast$ denotes the convolution operator. That is to say, the difference coarray of an N-element ULA is another ULA with $(2N - 1)$ elements. To achieve more DOFs, we can use the nested-array [29]. It is basically a concatenation of two ULAs, namely, inner and outer ULAs where they consist of N_1 and N_2 elements with spacing d_1 and spacing $d_2 = (N_1 + 1)d_1$, respectively. It is easily understood that the difference coarray of the two-level nested-array is a full ULA with $2N_2(N_1 + 1) - 1$ elements whose positions are

$$\{md_2, m = -N_e, -N_e + 1, \ldots, N_e,\ N_e = N_2(N_1 + 1) - 1\}. \tag{9}$$

This is a systematic way to increase the DOFs and the details can be found in [29]. An illustration for a two-level nested arrays with $N_1 = 3$ and $N_2 = 3$ is shown in Figure 1.

In summary, phased-MIMO enjoys increased transmit coherent gain at a cost of reduced DOFs. Since a ULA phased-array receiver is used in the basic phased-MIMO, we can use a nested-array as the receiver and thus increase the DOFs by difference coarray processing technique to compensate the DOF loss. This is just the motivation of this paper. The increased DOFs can be obtained when the nested-array is applied at the receiving end. Thus the DOF for phased-MIMO radar joints with nested-array as well as others can be shown as [29]. Comparing with (6a), (6b), and (6c), we can see that the proposed method is capable of proving $O(N^2)$ DOF from only $O(N)$ physical sensors and it is possible to get a dramatic increase in DOF:

$$\mathrm{DOF}_{\text{nested-pa-array}} = \frac{N^2}{2} + N + 1, \tag{10a}$$

$$\mathrm{DOF}_{\text{nested-pa-mimo}} = \frac{N^2 + 2N}{2} + 2K - 1, \tag{10b}$$

$$\mathrm{DOF}_{\text{nested-mimo}} = \frac{N^2 - 2}{2} + N + 2M. \tag{10c}$$

Table 1: Comparative DOF between the traditional method and the proposed method.

Method applied	Number of subarrays partitioned at the transmitting end	Number of sensors used at the receiving end	DOF
Traditional method	K	N	$O(N) + O(K)$
Proposed method	K	N	$O(N^2) + O(K)$

A comparison concerning DOF between the proposed method and the traditional method is summarized in Table 1.

From the foregoing analysis, by applying a new structure of "nested-array" on the receiving end, the proposed method can provide $O(N^2)$ degrees of freedom for a receiving end with N physical sensors. It also can be generated easily in a systematic mode. So the problem of detecting more sources than physical sensors can be addressed in this way.

3. Difference Coarray Processing Based Phased-MIMO Signal Model

Figure 2 compares our proposal of joint phased-MIMO and nested-array and the basic phased-MIMO, where the minimum element spacing d is assumed to be half of the wavelength. For analysis convenience, we rewrite (4) as a more general equation

$$\mathbf{y} = \sum_{i=1}^{L} \sqrt{\frac{M}{K}} \alpha_i \mathbf{u}(\theta_i) + \mathbf{n}, \tag{11}$$

where $L = D + 1$ is the number of sources including target and interferences. Multiplying both sides by $\sqrt{K/M}$, we have

$$\tilde{\mathbf{y}} = \mathbf{y}\sqrt{\frac{K}{M}} = \sum_{i=1}^{L} \alpha_i \mathbf{u}(\theta_i) + \sqrt{\frac{K}{M}}\mathbf{n} = \mathbf{U}\boldsymbol{\alpha} + \sqrt{\frac{K}{M}}\mathbf{n}, \tag{12}$$

where $\mathbf{U}$ denotes the virtual array manifold matrix and $\boldsymbol{\alpha} = [\alpha_1(\theta_1), \alpha_2(\theta_2), \ldots, \alpha_L(\theta_L)]^T$. It is easily understood that $\tilde{\mathbf{y}}$ satisfies the statistical model of $\tilde{\mathbf{y}} \sim N_c(\mu, \mathbf{R})$, where N_c stands for the complex multivariate circular Gaussian probability

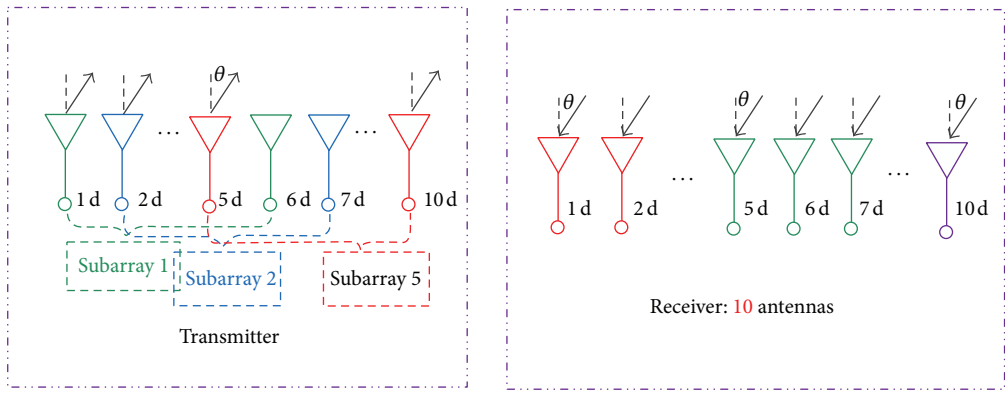

(a) Basic phased-MIMO

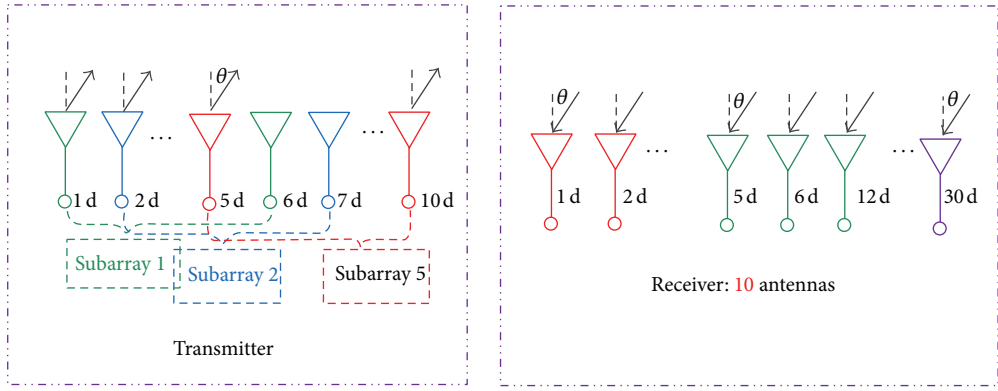

(b) Joint phased-MIMO and nested-array

Figure 2: Comparisons between our proposal of joint phased-MIMO and nested-array and the basic phased-MIMO.

density function, μ is the mean of $\tilde{\mathbf{y}}$, and $\mathbf{R}$ is its covariance matrix.

According to the difference coarray processing algorithm [32], we can get the autocorrelation matrix of $\tilde{\mathbf{y}}$ as

$$\begin{aligned}\mathbf{R}_{\tilde{y}\tilde{y}} &= E\left[\tilde{\mathbf{y}}\tilde{\mathbf{y}}^H\right] = E\left[\left(\mathbf{U}\boldsymbol{\alpha}+\sqrt{\frac{K}{M}}\mathbf{n}\right)\left(U\boldsymbol{\alpha}+\sqrt{\frac{K}{M}}\mathbf{n}\right)^H\right]\\ &= E\left[\left(\mathbf{U}\boldsymbol{\alpha}+\sqrt{\frac{K}{M}}\mathbf{n}\right)\left(\boldsymbol{\alpha}^H\mathbf{U}^H+\sqrt{\frac{K}{M}}\mathbf{n}^H\right)\right]\\ &= \mathbf{U}\begin{bmatrix}\sigma_1^2 & & & \\ & \sigma_2^2 & & \\ & & \cdots & \\ & & & \sigma_L^2\end{bmatrix}\mathbf{U}^H+\frac{K}{M}\sigma_n^2\mathbf{I},\end{aligned} \tag{13}$$

where superscript $(\cdot)^H$ denotes transpose conjugate and σ_n^2 is the noise variance. The corresponding original array manifold matrix $\mathbf{U}$ is given in (15).

Then we vectorize $\mathbf{R}_{\tilde{y}\tilde{y}}$ as the following vector:

$$\begin{aligned}\hat{\mathbf{y}} &= \operatorname{vec}\left(\mathbf{R}_{\tilde{y}\tilde{y}}\right) = \operatorname{vec}\left[\sum_{\mathbf{i}=\mathbf{1}}^{\mathbf{L}}\sigma_{\mathbf{i}}^2\mathbf{u}\left(\theta_{\mathbf{i}}\right)\mathbf{u}^{\mathbf{H}}\left(\theta_{\mathbf{i}}\right)\right]+\frac{\mathbf{K}}{\mathbf{M}}\sigma_{\mathbf{n}}^2\tilde{\mathbf{I}}_{\mathbf{n}}\\ &= \left(\mathbf{U}^*\oplus\mathbf{U}\right)\mathbf{p}+\frac{K}{M}\sigma_n^2\vec{\mathbf{I}}_n,\end{aligned} \tag{14}$$

where the sources power vector $\mathbf{p} = [\sigma_1^2, \sigma_2^2, \ldots, \sigma_L^2]^T$ and $\vec{\mathbf{I}}_n = [\mathbf{e}_1^T, \mathbf{e}_2^T, \ldots, \mathbf{e}_N^T]^T$ whose element $\mathbf{e}_i$ stands for a column vector of all zeros except a 1 at the ith position. And the symbol $\oplus$ is used to denote the Khatri Rao (KR) product. Also, the new virtual array manifold $\mathbf{U}^* \oplus \mathbf{U}$ is derived in (16). Both of (15) and (16) are shown at bottom of the next page. We can see that the dimension of the new virtual array manifold $\mathbf{U}^* \oplus \mathbf{U}$ is $KN^2 \times L$. Obviously, the equivalent aperture has been significantly increased. More importantly, it is a ULA virtual array. Here, we can view $\hat{\mathbf{y}}$ as the observation vector comparing with (11). And $\mathbf{p}$ which consists of the sources' powers represents the equivalent source signal vector.

Now we would like to consider the computation complexity of this proposed method. From (14), we can see that

K^2N^4L complex multiplication and $KN^2(L-1)$ addition of complex quantities have been increased. These considerations reveal that the complexity of the proposal is of $O(K^2N^4L)$. Due to the difference coarray processing, it takes much resources to compute the autocorrelation matrix of the received data and is beneficial for us to make full use of the statistics:

$$\mathbf{U} = [\mathbf{u}(\theta_1), \ldots, \mathbf{u}(\theta_L)] = \begin{pmatrix} e^{-j(2\pi/\lambda)(d_{t1}+d_{r1})\sin(\theta_1)} & \cdots & e^{-j(2\pi/\lambda)(d_{t1}+d_{r1})\sin(\theta_i)} & \cdots & e^{-j(2\pi/\lambda)(d_{t1}+d_{r1})\sin(\theta_L)} \\ \vdots & & \vdots & & \vdots \\ e^{-j(2\pi/\lambda)(d_{t1}+d_{rN})\sin(\theta_1)} & \cdots & e^{-j(2\pi/\lambda)(d_{t1}+d_{rN})\sin(\theta_i)} & \cdots & e^{-j(2\pi/\lambda)(d_{t1}+d_{rN})\sin(\theta_L)} \\ \vdots & & \vdots & & \vdots \\ e^{-j(2\pi/\lambda)(d_{tK}+d_{r1})\sin(\theta_1)} & \cdots & e^{-j(2\pi/\lambda)(d_{tK}+d_{r1})\sin(\theta_i)} & \cdots & e^{-j(2\pi/\lambda)(d_{tK}+d_{r1})\sin(\theta_L)} \\ \vdots & & \vdots & & \vdots \\ e^{-j(2\pi/\lambda)(d_{tK}+d_{rN})\sin(\theta_1)} & \cdots & e^{-j(2\pi/\lambda)(d_{tK}+d_{rN})\sin(\theta_i)} & \cdots & e^{-j(2\pi/\lambda)(d_{tK}+d_{r1})\sin(\theta_L)} \end{pmatrix}_{KN\times L}, \tag{15}$$

$$\mathbf{U}^* \oplus \mathbf{U} = \begin{pmatrix} e^{-j(2\pi/\lambda)(d_{t1}+d_{r1}-d_{t1}-d_{r1})\sin(\theta_1)} & \cdots & e^{-j(2\pi/\lambda)(d_{t1}+d_{r1}-d_{t1}-d_{r1})\sin(\theta_i)} & \cdots & e^{-j(2\pi/\lambda)(d_{t1}+d_{r1}-d_{t1}-d_{r1})\sin(\theta_L)} \\ \vdots & & \vdots & & \vdots \\ e^{-j(2\pi/\lambda)(d_{tK}+d_{rN}-d_{t1}-d_{r1})\sin(\theta_1)} & \cdots & e^{-j(2\pi/\lambda)(d_{tK}+d_{rN}-d_{t1}-d_{r1})\sin(\theta_i)} & \cdots & e^{-j(2\pi/\lambda)(d_{tK}+d_{rN}-d_{t1}-d_{r1})\sin(\theta_L)} \\ \vdots & & \vdots & & \vdots \\ e^{-j(2\pi/\lambda)(d_{t1}+d_{r1}-d_{tK}-d_{rN})\sin(\theta_1)} & \cdots & e^{-j(2\pi/\lambda)(d_{t1}+d_{r1}-d_{tK}-d_{rN})\sin(\theta_i)} & \cdots & e^{-j(2\pi/\lambda)(d_{t1}+d_{r1}-d_{tK}-d_{rN})\sin(\theta_L)} \\ \vdots & & \vdots & & \vdots \\ e^{-j(2\pi/\lambda)(d_{tK}+d_{rN}-d_{tK}-d_{rN})\sin(\theta_1)} & \cdots & e^{-j(2\pi/\lambda)(d_{tK}+d_{rN}-d_{tK}-d_{rN})\sin(\theta_i)} & \cdots & e^{-j(2\pi/\lambda)(d_{tK}+d_{rN}-d_{tK}-d_{rN})\sin(\theta_L)} \end{pmatrix}_{KN^2\times L}. \tag{16}$$

For simplicity and without loss of generality, firstly we consider a special example where all subarrays have an equal aperture. In this case, the nonadaptive transmit beamformer weight vectors are given by

$$\mathbf{w}_k = \frac{\mathbf{a}_k(\theta_s)}{\|\mathbf{a}_k(\theta_s)\|}, \quad k = 1, 2, \ldots, K. \tag{17}$$

Correspondingly, the normalized transmit coherent processing vector $\mathbf{c}(\theta_s)$ can be expressed as

$$\begin{aligned} \mathbf{c}(\theta_s) &= \left[\frac{\mathbf{a}_1^H(\theta_s)\,\mathbf{a}_1(\theta_s)}{\|\mathbf{a}_1(\theta_s)\|}, \ldots, \frac{\mathbf{a}_K^H(\theta_s)\,\mathbf{a}_K(\theta_s)}{\|\mathbf{a}_K(\theta_s)\|}\right]^T \\ &= \left[\sqrt{M-K+1}, \ldots, \sqrt{M-K+1}\right]^T. \end{aligned} \tag{18}$$

We then have

$$\mathbf{c}(\theta_s) \odot \mathbf{d}(\theta_s) = \sqrt{M-K+1}\left[e^{-j\tau_1(\theta_s)}, \ldots, e^{-j\tau_K(\theta_s)}\right]^T. \tag{19}$$

Substituting it to (5) yields

$$\begin{aligned} &\mathbf{u}(\theta_s) \\ &= (\mathbf{c}(\theta_s) \odot \mathbf{d}(\theta_s)) \otimes \mathbf{b}(\theta_s) \\ &= \sqrt{M-K+1}\left[e^{-j(2\pi/\lambda)d_{t1}\sin(\theta_s)}, \ldots, e^{-j(2\pi/\lambda)d_{tK}\sin(\theta_s)}\right]^T \\ &\quad \otimes \left[e^{-j(2\pi/\lambda)d_{r1}\sin(\theta_s)}, \ldots, e^{-j(2\pi/\lambda)d_{rN}\sin(\theta_s)}\right]^T \\ &= \sqrt{M-K+1}\left[e^{-j(2\pi/\lambda)(d_{t1}+d_{r1})\sin(\theta_s)}, \ldots,\right. \\ &\qquad e^{-j(2\pi/\lambda)(d_{t1}+d_{rN})\sin(\theta_s)}, \\ &\qquad e^{-j(2\pi/\lambda)(d_{t2}+d_{r1})\sin(\theta_s)}, \ldots, \\ &\qquad e^{-j(2\pi/\lambda)(d_{t2}+d_{rN})\sin(\theta_s)}, \ldots, \\ &\qquad e^{-j(2\pi/\lambda)(d_{tK}+d_{r1})\sin(\theta_s)}, \ldots, \\ &\qquad \left. e^{-j(2\pi/\lambda)(d_{tK}+d_{rN})\sin(\theta_s)}\right]^T. \end{aligned} \tag{20}$$

4. Adaptive Beamforming

In order to maximize the output signal-plus-noise ratios (SINR), adaptive beamforming should be employed. Applying the beamformer weighter $\mathbf{w}_p$ to (14), we can get

$$\begin{aligned}\widetilde{Y} &= \mathbf{w}_p^H \widehat{\mathbf{y}} = \sum_{i=1}^{L} \mathbf{w}_p^H \left[\mathbf{u}^* \left(\theta_i\right) \otimes \mathbf{u}\left(\theta_i\right)\right] \sigma_i^2 + \frac{K}{M}\sigma_n^2 \mathbf{w}_p^H \vec{\mathbf{I}}_n \\ &= \sum_{i=1}^{L} \mathbf{B}_{\text{power}}\left(\theta_i\right)\sigma_i^2 + \frac{K}{M}\sigma_n^2 \mathbf{w}_p^H \vec{\mathbf{I}}_n,\end{aligned} \tag{21}$$

where $\mathbf{B}_{\text{power}}(\theta) = \mathbf{w}_p^H[\mathbf{u}^*(\theta) \otimes \mathbf{u}(\theta)]$. Equation (21) means that, though the incident interferences are originally assumed uncorrelated, after the difference coarray processing, they are represented by their powers vector $\mathbf{p}$ which consists of the powers σ_i^2 in (14) and they behave like fully coherent sources. Consequently the resulting covariance matrix of the observation vector $\widehat{\mathbf{y}}$ will be of rank 1. For the fact that the classic minimum variance distortionless response (MVDR) technique yields poor performance when the jammers are coherent, so the MVDR cannot be applied directly on $\widehat{\mathbf{y}}$ for the beamforming. To address this problem, we perform spatial smoothing on $\widehat{\mathbf{y}}$ as follows.

(i) First, we construct a new matrix $\mathbf{U}_1$ of size $((N^2 - 2)/2 + N + 2K) \times L$ from the $\mathbf{U}^* \oplus \mathbf{U}$, where the repeated rows (after their first occurrence) have been removed.

(ii) The elements in $\mathbf{U}_1$ are sorted, so that the ith row corresponds to the sensor location $(N^2/4 + N/2 + K - 1 + i)d$ in the difference coarray of the original virtual array. This is equivalent to removing the corresponding rows from the observation vector $\widehat{\mathbf{y}}$ and sorting them to get a new vector $\widehat{\mathbf{y}}_1$ given by

$$\widehat{\mathbf{y}}_1 = \mathbf{U}_1 \mathbf{p} + \frac{K}{M}\sigma_n^2 \vec{\mathbf{e}}', \tag{22}$$

where $\vec{\mathbf{e}}' \in \mathbb{R}^{(2(N+K-1)-1)\times 1}$ is a vector of all zeros except a 1 at the $(N + K - 1)$th position. After the sorting and replacement of repeated rows, the deterministic noise vector $\vec{\mathbf{I}}_n$ in (14) has been changed to $\vec{\mathbf{e}}'$ and the difference coarray of the original virtual array has equivalent elements located from $(-N^2/4 - N/2 - K + 1)d$ to $(N^2/4 + N/2 + K - 1)d$.

(iii) We now divide this difference coarray into $(N^2/4 + N/2 + K)$ overlapping subarrays, each with $(N^2/4 + N/2 + K)$ elements, where the ith subarray has the elements corresponding to the $(N^2/4 + N/2 + K - 1 - i)$th to $((N^2 - 2)/2 + N + 2K - 2 - i)$th rows of $\widehat{\mathbf{y}}_1$, which we denote by $\widehat{\mathbf{y}}_{1i} = \mathbf{U}_{1i}\mathbf{p} + (K/M)\sigma_n^2 \mathbf{e}_i'$. The $\mathbf{U}_{1i}$ is a $(N^2/4 + N/2 + K - 1) \times L$ matrix consisting of the $(N^2/4 + N/2 + K - 1 - i)$th to $((N^2 - 2)/2 + N + 2K - 2 - i)$th rows of $\mathbf{U}_1$ and $\mathbf{e}_i'$ is a vector of all zeros expect a 1 at the ith position. It is easy to prove that

$$\widehat{\mathbf{y}}_{1i} = \mathbf{U}_{11}\mathbf{\Phi}^{i-1}\mathbf{p} + \frac{K}{M}\sigma_n^2 \mathbf{e}_i', \tag{23}$$

where

$$\mathbf{\Phi} = \begin{pmatrix} e^{-j(2\pi/\lambda)d\sin(\theta_1)} & & & \\ & e^{-j(2\pi/\lambda)d\sin(\theta_2)} & & \\ & & \ddots & \\ & & & e^{-j(2\pi/\lambda)d\sin(\theta_L)} \end{pmatrix}. \tag{24}$$

(iv) The covariance matrix of $\widehat{\mathbf{y}}_{1i}$ is

$$\begin{aligned}\mathbf{R}_i &= E\left\{\widehat{\mathbf{y}}_{1i}\widehat{\mathbf{y}}_{1i}^{\mathbf{H}}\right\} \\ &= \mathbf{U}_{11}\mathbf{\Phi}^{i-1}\mathbf{p}\mathbf{p}^H{\mathbf{\Phi}^{i-1}}^H\mathbf{U}_{11}^H + \frac{K^2}{M^2}\sigma_n^2 \mathbf{e}_i'{\mathbf{e}_i'}^H \\ &\quad + \frac{K}{M}\sigma_n^2 \mathbf{U}_{11}\mathbf{\Phi}^{i-1}\mathbf{p}{\mathbf{e}_i'}^H + \frac{K}{M}\sigma_n^2 \mathbf{e}_i'\mathbf{p}^H{\mathbf{\Phi}^{i-1}}^H\mathbf{U}_{11}^H.\end{aligned} \tag{25}$$

The spatially smoothed covariance matrix $\mathbf{R}_{\text{ss}}$ can then be obtained by taking the average of $\mathbf{R}_i$ over all i:

$$\mathbf{R}_{\text{ss}} \triangleq \frac{1}{N + K - 1}\sum_{i=1}^{N+K-1} \mathbf{R}_i. \tag{26}$$

(v) The $\mathbf{R}_{\text{ss}}$ enables us to build a full rank covariance matrix which can be applied for performing MVDR beamforming on the received data of the joint phased-MIMO and nested-array. For instance, using the subarray with elements at nd, $n = 0, 1, \ldots, (N^2/4 + N/2 + K - 1)$ as the reference subarray (we denote its steering vector as $\mathbf{a}_1(\theta)$), the MVDR beamform weighter can then be derived as

$$\mathbf{w}_p = \frac{\mathbf{R}_{\text{ss}}^{-1}\mathbf{a}_1\left(\theta_s\right)}{\mathbf{a}_1\left(\theta_s\right)^H \mathbf{R}_{\text{ss}}^{-1}\mathbf{a}_1\left(\theta_s\right)}. \tag{27}$$

Finally, the eigen decomposition of $\mathbf{R}_{\text{ss}}$ is

$$\mathbf{R}_{\text{ss}} = \mathbf{E}_s\mathbf{\Lambda}_s\mathbf{E}_s^H + \mathbf{E}_n\mathbf{\Lambda}_n\mathbf{E}_n^H, \tag{28}$$

where the diagonal matrix $\mathbf{\Lambda}_s$ contains the L target eigenvalues and the columns of $\mathbf{E}_s$ are the corresponding eigenvectors, while the diagonal matrix $\mathbf{\Lambda}_n$ contains the remaining $N^2/4 - N/2 + K - L$ eigenvalues and the columns of $\mathbf{E}_n$ are the corresponding eigenvectors constructing the noise space. The DOA of targets can then be estimated from the peaks of the multiple signal classification (MUSIC) spectra

$$\mathbf{z}\left(\theta\right) = \frac{\mathbf{a_1^H}\left(\theta\right)\mathbf{a_1}\left(\theta\right)}{\mathbf{a_1^H}\left(\theta\right)\mathbf{P}\mathbf{a_1}\left(\theta\right)}, \tag{29}$$

where $\mathbf{P} = \mathbf{E}_n\mathbf{E}_n^H = \mathbf{I} - \mathbf{E}_s\mathbf{E}_s^H$ is the projection matrix onto the noise subspace.

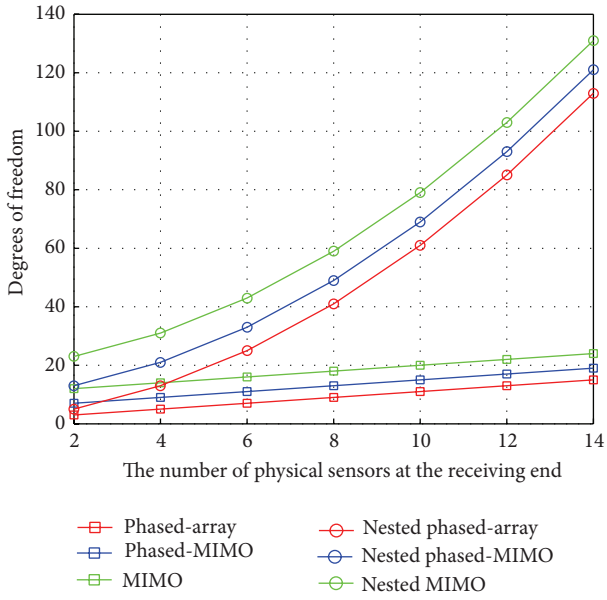

FIGURE 3: Comparative DOF versus sensors' number.

5. Simulation Results

Throughout our simulations, we assume a ULA of $M = 10$ omnidirectional antennas used for transmitting the based-band waveforms $\{\phi_k(t) = Q(T_0)\exp^{j2\pi(k/T_0)t}\}_{k-1}^{K}$, where $Q(T_0) = \sqrt{1/T_0}$ and $K = 5$. $N = 10$ omnidirectional receiving phased-array elements are used in the simulations, except Example 2 where $N = 5$ is used. The additive Gaussian white noise is assumed to be zero-mean and unit-variance. All the statistical results are computed based on 300 independent runs.

5.1. DOF Comparison. Firstly, we would like to demonstrate the superior capability of the proposal which can provide a dramatic increase in the DOF. We compare the phased-MIMO technique with the phased-array and the MIMO radar when the nested-array structure is applied at the receiving end. According to the relationship concerning DOF and the number of sensors obtained in Section 2, the notable difference can be shown in Figure 3. It can be seen from the figure that the proposal obtains much more DOF than the traditional method. Moreover, as the number of physical sensors increases, the difference between proposal and the traditional method tends to increase. On the other hand, the MIMO radar exhibits DOF performance which is better than two other techniques. Because the transmit array of the MIMO radar is divided into M subarrays which is the most subarrays. The main drawback of MIMO radar is that it sacrifices the coherent processing gain as compared to phased-MIMO technique.

5.2. Adaptive Beamforming. Suppose a target of interest is located at 10° and eight interferences located at {−50°, −30°, −20°, 0°, 15°, 30°, 50°, 60°}. The target power is fixed to 0 dB

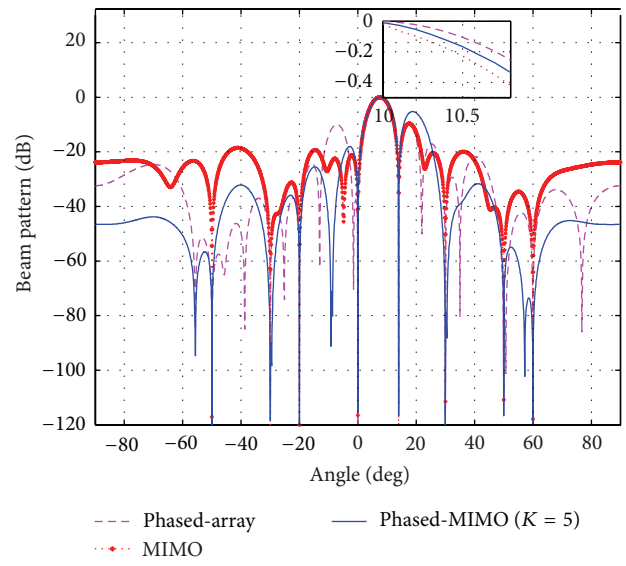

(a) Basic phased-MIMO

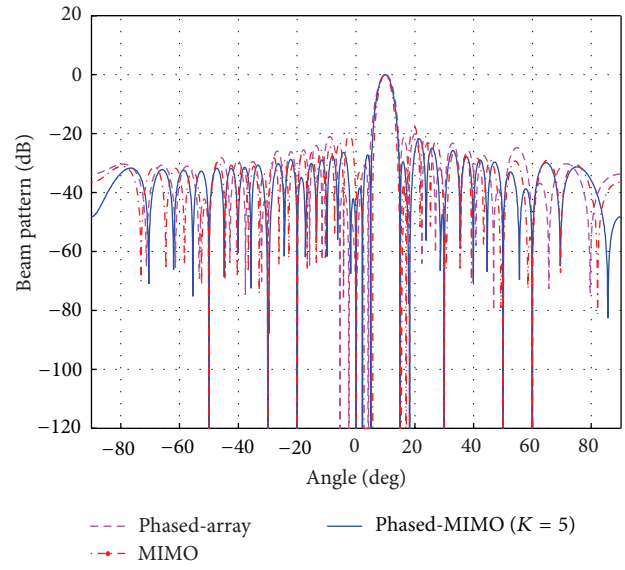

(b) Joint phased-MIMO and nested-array

FIGURE 4: Comparative MVDR beam pattern when $D = 8$.

while the interference power is fixed to 50 dB. Figure 4 compares the MVDR beam pattern between the basic phased-MIMO and our proposal of joint phased-MIMO and nested-array. The comparison between Figures 4(a) and 4(b) suggests that our proposal yields significant performance improvements such as much narrower main beamwidth and lower sidelobe levels. From the amplifying subgraph in Figure 4(a), we can see that there are some difference for the width of the main lobe among the three different techniques. Also, we can notice that both of the MIMO ($K = M = 10$) and phased-MIMO ($K = 5$) offer lower sidelobe levels than the phased-array ($K = 1$). More importantly, our proposal can offer more notches. This means that more interferences can be effectively suppressed or more targets can be identified.

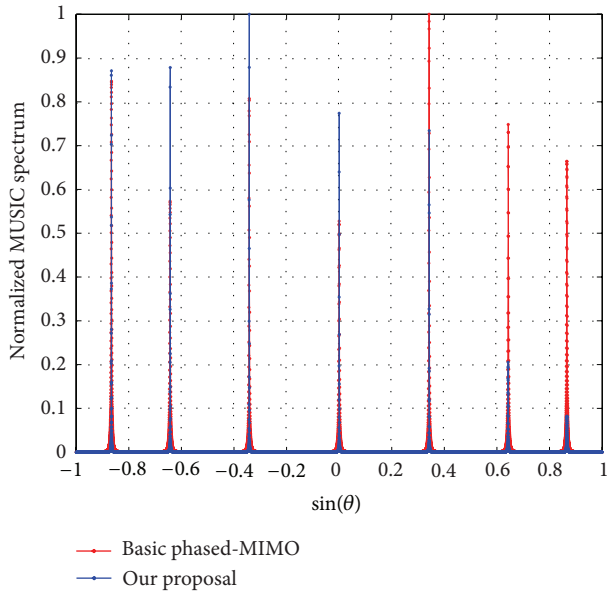

Figure 5: Comparative MUSIC spectra when $L = 7$.

5.3. DOA Estimation. Here, we provide two examples to show the superior performance of our proposal.

Example 1. Consider $N = 10$. First, we consider 7 sources with the DOAs of $\{-60^\circ, -40^\circ, -20^\circ, 0^\circ, 20^\circ, 40^\circ, 60^\circ\}$ and the signal-to-noise (SNR) is assumed to be 0 dB. Figure 5 compares the MUSIC spectra of our proposal to the basic phased-MIMO. We can see that both of them can resolve the 7 targets clearly. This is because they can resolve up to $(N + K - 1)$ and $(N^2/4 + N/2 + K - 1)$ sources, respectively. Therefore, our proposal can resolve more sources. For instance, Figure 6 compares the MUSIC spectra when there are $L = 14$ and $L = 27$ sources, respectively. Obviously, the basic phased-MIMO fails to detect many sources, but our proposal reveals a superior performance with more clearly discernible peaks of the MUSIC spectra.

Example 2. Consider $N = 5$. Furthermore, we consider an alternative receive array by reducing the $N = 10$ elements to $N = 5$ elements. The elements are arranged as Figure 7, where the receiving elements are located in receiver as a vector $[1, 0, 1, 0, 0, 1, 0, 0, 1, 1]$. Here 1 means that the antenna with an index corresponding to the location of that 1 in the vector belongs to the receive array while 0 means it does not. Suppose also that there are 7 targets with the DOAs of $\{-60^\circ, -40^\circ, -20^\circ, 0^\circ, 20^\circ, 40^\circ, 60^\circ\}$. Figure 8 compares this alternative arrangement with the basic phased-MIMO that still keeps the $N = 10$ elements in the receiver (see Figure 2). It is noticed that both of the two arrangements can resolve the 7 sources sufficiently well, but our proposal uses only 5 elements in the receiver whereas 10 elements are used in the basic phased-MIMO to get an equivalent performance.

It is necessary to analyze the RMSE performance. Suppose there is one source located at 30°. The system parameters

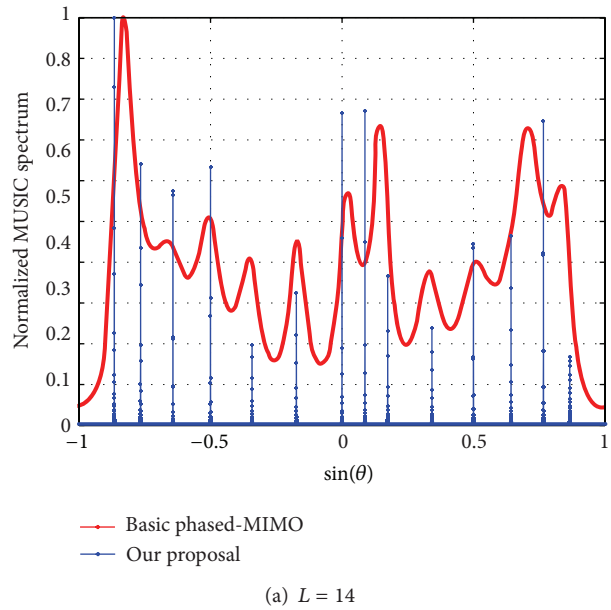

(a) $L = 14$

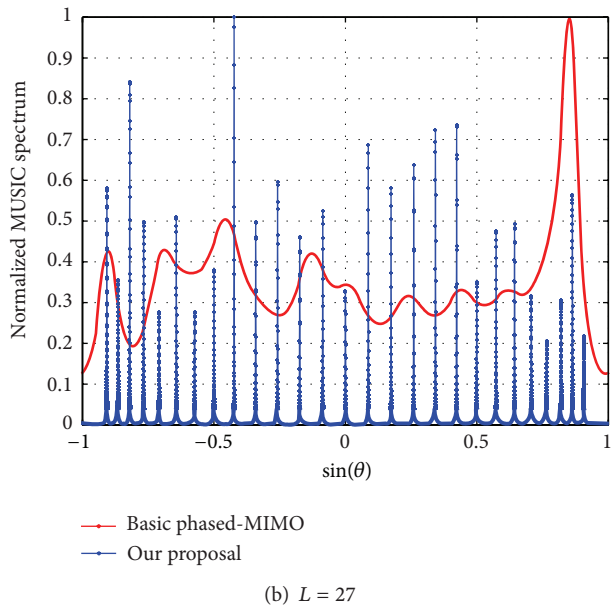

(b) $L = 27$

Figure 6: DOF comparisons in MUSIC spectra.

used in Examples 1 and 2 are simulated, respectively. Their comparative RMSE versus SNR results are given in Figures 9 and 10. We can see that our proposal achieves much better performance than the basic phased-MIMO.

6. Conclusion

In this paper, we propose a joint phased-MIMO and nested-array for increased DOFs to resolve more sources. The essence of the proposal is to apply the difference coarray processing to the joint phased-MIMO and nested-array to generate more virtual array elements. Additionally, a spatial

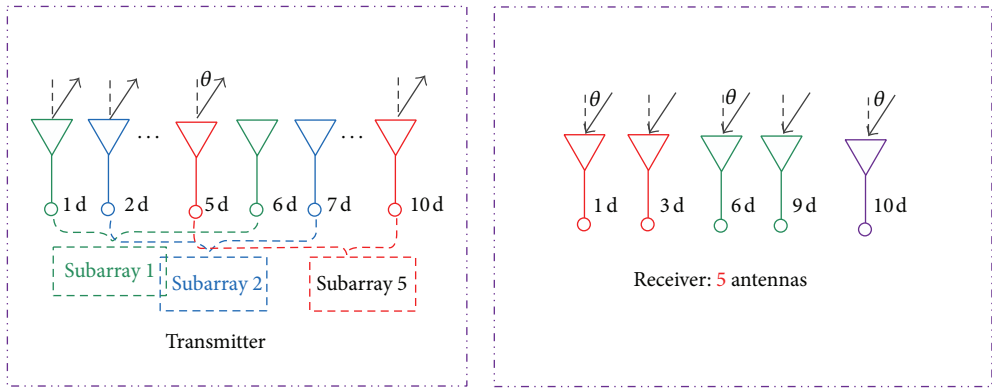

Figure 7: Alternative receiving array with 5 elements for joint phased-array and nested-array.

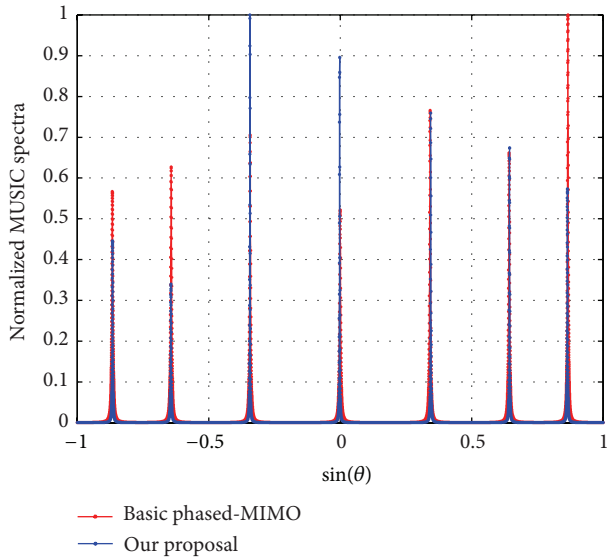

Figure 8: Comparative MUSIC spectra for the alternative receiving array.

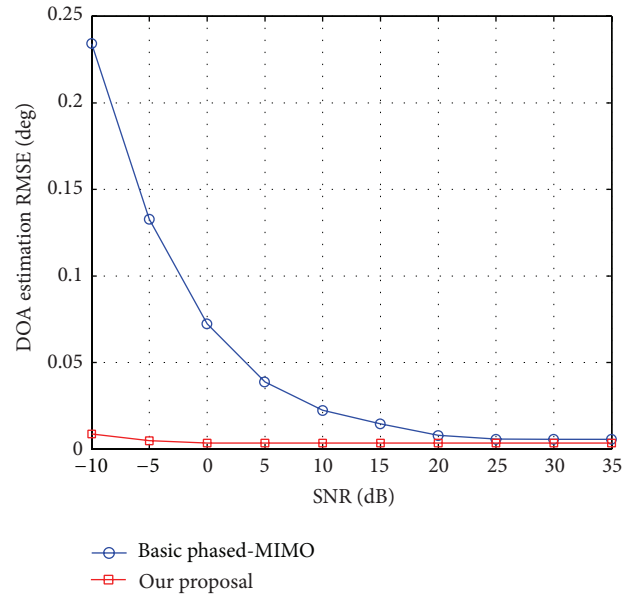

Figure 9: Comparative RMSE versus SNR for Example 1.

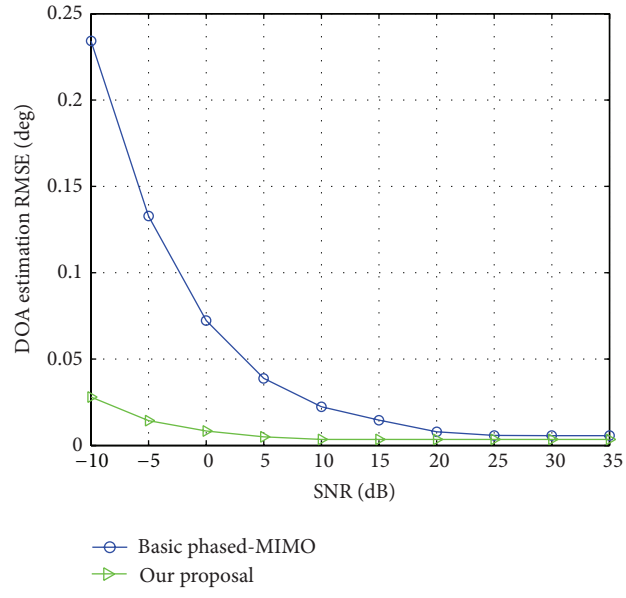

Figure 10: Comparative RMSE versus SNR for Example 2.

smoothing algorithm is used to overcome the interference coherent problem in the difference coarray data. Extensive simulation results show that our proposal allows to achieve more DOFs and better source localization performance. Meanwhile, our proposal yields superior DOA estimation RMSE performance. In our proposed design, the real array element spacing is integer multiple of half-wavelength. The spacing is implementable in practical array systems. However, coupling is ignored in the algorithm development. As a future work, we will study the coupling effects and other physical realizability issues. Another research direction is to extend the linear array to other arrays.

Conflict of Interests

The authors declare that there is no conflict of interests regarding the publication of this paper.

Acknowledgments

The work described in this paper was supported by the National Natural Science Foundation of China under Grant 41101317, the Program for New Century Excellent Talents in University under Grant NCET-12-0095, and Sichuan Province Science Fund for Distinguished Young Scholars under Grant 2013JQ0003.

References

[1] C. Redondo and L. de Haro, "On the analysis and design of reconfigurable multimode MIMO microstrip antennas," *IEEE Transactions on Antennas and Propagation*, vol. 62, no. 1, pp. 119–129, 2014.

[2] W.-Q. Wang, "Large-area remote sensing in high-altitude high-speed platform Using MIMO SAR," *IEEE Journal of Selected Topics in Applied Earth Observations and Remote Sensing*, vol. 6, no. 5, pp. 2146–2158, 2013.

[3] L. Liu, S. W. Cheung, and T. I. Yuk, "Compact MIMO antenna for portable devices in UWB applications," *IEEE Transactions on Antennas and Propagation*, vol. 61, no. 8, pp. 4257–4264, 2013.

[4] O. N. Alrabadi, J. Perruisseau-Carrier, and A. Kalis, "MIMO transmission using a single RF source: theory and antenna design," *IEEE Transactions on Antennas and Propagation*, vol. 60, no. 2, pp. 654–664, 2012.

[5] M. Webb, M. Q. Yu, and M. Beach, "Propagation characteristics, metrics, and statistics for virtual MIMO performance in a measured outdoor cell," *IEEE Transactions on Antennas and Propagation*, vol. 59, no. 1, pp. 236–244, 2011.

[6] W.-Q. Wang, "Virtual antenna array analysis for MIMO synthetic aperture radars," *International Journal of Antennas and Propagation*, vol. 2012, Article ID 587276, 10 pages, 2012.

[7] M. Contu and P. Lombardo, "Sidelobe control for a MIMO radar virtual array," in *Proceedings of the IEEE Radar Conference*, pp. 1–6, Ottawa, Canada, May 2013.

[8] S. Sugiura, "Coherent versus non-coherent reconfigurable antenna aided virtual MIMO systems," *IEEE Signal Processing Letters*, vol. 21, no. 4, pp. 390–394, 2014.

[9] A. Hassanien and S. A. Vorobyov, "Phased-MIMO radar: a tradeoff between phased-array and MIMO radars," *IEEE Transactions on Signal Processing*, vol. 58, no. 6, pp. 3137–3151, 2010.

[10] D. R. Fuhrmann, J. P. Browning, and M. Rangaswamy, "Signaling strategies for the hybrid MIMO phased-array radar," *IEEE Journal on Selected Topics in Signal Processing*, vol. 4, no. 1, pp. 66–78, 2010.

[11] H. Li and B. Himed, "Transmit subaperturing for MIMO radars with co-located antennas," *IEEE Journal on Selected Topics in Signal Processing*, vol. 4, no. 1, pp. 55–65, 2010.

[12] W.-Q. Wang and H. C. So, "Transmit subaperturing for range and angle estimation in frequency diverse array radar," *IEEE Transactions on Signal Processing*, vol. 62, no. 8, pp. 2000–2011, 2014.

[13] S. U. Pillai, Y. B. Ness, and F. Haber, "A new approach to array geometry for improved spatial spectrum estimation," *Proceedings of the IEEE*, vol. 73, no. 10, pp. 1522–1524, 1985.

[14] A. Moffet, "Minimum-redundancy linear arrays," *IEEE Transactions on Antennas and Propagation*, vol. 16, no. 2, pp. 172–175, 1968.

[15] J. Dong, Q. X. Li, and W. Guo, "A combinatorial method for antenna array design in minimum redundancy MIMO radars," *IEEE Antennas and Wireless Propagation Letters*, vol. 8, pp. 1150–1153, 2009.

[16] G. Oliveri, F. Caramanica, M. D. Migliore, and A. Massa, "Synthesis of nonuniform MIMO arrays through combinatorial sets," *IEEE Antennas and Wireless Propagation Letters*, vol. 11, no. 11, pp. 728–731, 2012.

[17] W. Roberts, L. Z. Xu, J. Li, and P. Stoica, "Sparse antenna array design for MIMO active sensing applications," *IEEE Transactions on Antennas and Propagation*, vol. 59, no. 3, pp. 846–858, 2011.

[18] N. Hu, Z. F. Ye, X. Xu, and M. Bao, "DOA estimation for sparse array via sparse signal reconstruction," *IEEE Transactions on Aerospace and Electronic Systems*, vol. 49, no. 2, pp. 760–773, 2013.

[19] L. F. Yepes, D. H. Covarrubias, M. A. Alonso, and R. Ferrus, "Hybrid sparse linear array synthesis applied to phased antenna arrays," *IEEE Antennas and Wireless Propagation Letters*, vol. 13, pp. 185–188, 2014.

[20] A. A. Khan and A. K. Brown, "Null steering in irregularly spaced sparse antenna arrays using aperture distributed subarrays and hybrid optimiser," *IET Microwaves, Antennas and Propagation*, vol. 8, no. 2, pp. 86–92, 2014.

[21] O. M. Bucci, T. Isernia, and A. F. Morabito, "An effective deterministic procedure for the synthesis of shaped beams by means of uniform-amplitude linear sparse arrays," *IEEE Transactions on Antennas and Propagation*, vol. 61, no. 1, pp. 169–175, 2013.

[22] L. Cen, Z. L. Yu, W. Ser, and W. Cen, "Linear aperiodic array synthesis using an improved genetic algorithm," *IEEE Transactions on Antennas and Propagation*, vol. 60, no. 2, part 2, pp. 895–902, 2012.

[23] G. Oliveri and A. Massa, "Genetic algorithm (GA)-enhanced almost difference set (ADS)-based approach for array thinning," *IET Microwaves, Antennas & Propagation*, vol. 5, no. 3, pp. 305–315, 2011.

[24] L. Carin, D. H. Liu, and B. Guo, "Coherence, compressive sensing, and random sensor arrays," *IEEE Antennas and Propagation Magazine*, vol. 53, no. 4, pp. 28–39, 2011.

[25] S. Holm, B. Elgetun, and G. Dahl, "Properties of the beampattern of weight- and layout-optimized sparse arrays," *IEEE Transactions on Ultrasonics, Ferroelectrics, and Frequency Control*, vol. 44, no. 5, pp. 983–991, 1997.

[26] G. Oliveri, M. Carlin, and A. Massa, "Complex-weight sparse linear array synthesis by Bayesian compressive sampling," *IEEE Transactions on Antennas and Propagation*, vol. 60, no. 5, pp. 2309–2326, 2012.

[27] F. Viani, G. Oliveri, and A. Massa, "Compressive sensing pattern matching techniques for synthesizing planar sparse arrays," *IEEE Transactions on Antennas and Propagation*, vol. 61, no. 9, pp. 4577–4587, 2013.

[28] G. Oliveri and A. Massa, "ADS-based array design for 2-D and 3-D ultrasound imaging," *IEEE Transactions on Ultrasonics, Ferroelectrics, and Frequency Control*, vol. 57, no. 7, pp. 1568–1582, 2010.

[29] P. Pal and P. P. Vaidyanathan, "Nested arrays: a novel approach to array processing with enhanced degrees of freedom," *IEEE Transactions on Signal Processing*, vol. 58, no. 8, pp. 4167–4181, 2010.

[30] P. Pal and P. P. Vaidyanathan, "A novel array structure for directions-of-arrival estimation with increased degrees of freedom," in *Proceedings of the IEEE International Conference on Acoustics, Speech, and Signal Processing (ICASSP '10)*, pp. 2606–2609, IEEE, Dallas, Tex, USA, March 2010.

[31] P. Pal and P. P. Vaidyanathan, "Beamforming using passive nested arrays of sensors," in *Proceedings of the IEEE International Symposium on Circuits and Systems: Nano-Bio Circuit Fabrics and Systems (ISCAS '10)*, pp. 2840–2843, Paris, France, June 2010.

[32] R. T. Hoctor and S. A. Kassam, "Unifying role of the coarray in aperture synthesis for coherent and incoherent imaging," *Proceedings of the IEEE*, vol. 78, no. 4, pp. 735–752, 1990.

[33] D. Nion and N. D. Sidiropoulos, "A PARAFAC-based technique for detection and localization of multiple targets in a MIMO radar system," in *Proceedings of the IEEE International Conference on Acoustics, Speech, and Signal Processing (ICASSP '09)*, pp. 2077–2080, Taipei, Taiwan, April 2009.

[34] W.-Q. Wang, "Phased-MIMO radar with frequency diversity for range-dependent beamforming," *IEEE Sensors Journal*, vol. 13, no. 4, pp. 1320–1328, 2013.